



PERGAMON

Atmospheric Environment 35 (2001) 2231–2242

ATMOSPHERIC  
ENVIRONMENT

www.elsevier.com/locate/atmosenv

# Use of the Kit Fox field data to analyze dense gas dispersion modeling issues

Steven R. Hanna<sup>a,\*</sup>, Joseph C. Chang<sup>b</sup>

<sup>a</sup>CSI Mail Stop 5C3, 103 Science and Technology I, George Mason University, 4400 University Drive, Fairfax, VA 22030-4444, USA

<sup>b</sup>Earth Tech, Inc., 196 Baker Avenue, Concord, MA 01742, USA

Received 19 April 2000; received in revised form 6 October 2000; accepted 11 October 2000

## Abstract

The 1995 Kit Fox dense gas field data set consists of 52 trials where short-duration CO<sub>2</sub> gas releases were made at ground level over a rough surface during neutral to stable conditions. The experiments were intended to demonstrate the effects on dense gas clouds of relatively large roughnesses typical of industrial process plants. Fast response concentration observations were made by 80 samplers located on four downwind lines (25, 50, 100, and 225 m), including profile observations on three towers on each of the closest three arcs. Detailed meteorological measurements were made on several towers within and outside of the roughness arrays. The data analysis emphasized the variation of maximum concentration with surface roughness, the dependence of cloud advection speed on cloud depth, the variation of the three components of dispersion with ambient turbulence, and the dependence of vertical entrainment rate on ambient friction velocity and cloud Richardson number. The Kit Fox data were used to evaluate a specific dense gas dispersion model (HEGADAS 3+), with emphasis on whether it would be able to account for the increased roughness. The model was able to satisfactorily simulate the observed concentrations, with a mean bias of about 5% and with about 90% of the predictions within a factor of two of the observations. © 2001 Elsevier Science Ltd. All rights reserved.

*Keywords:* Dispersion; Dense gases; Kit Fox dense gas experiment; Model evaluation

## 1. Introduction and objectives

The Kit Fox dense gas field experiment was part of the Petroleum Environmental Research Forum (PERF) 93-16 atmospheric dispersion modeling study which has been discussed in the previous six papers in this special issue. Hanna and Steinberg (2001) give an overview of the study. The Kit Fox experiment was carried out in late summer 1995 at the US Department of Energy (DOE) Nevada Test Site. Dense gas (CO<sub>2</sub>, with density about 1.5 times that of air) was released at ground level for 2–5 min periods (continuous “plumes”) and for 20 s

periods (short-duration transient “puffs”), including both neutral and stable conditions. The desert surface, a dry lake bed known as Frenchman Flat, was artificially roughened using combinations of flat billboard obstacles in order to simulate the roughness of an industrial site and its surroundings at about 1/10 scale.

Until the Kit Fox field experiment took place, most field and wind tunnel studies of dense gas dispersion involved idealized experiments in which the source emissions were either continuous or instantaneous (i.e., not transient), the underlying surface was relatively smooth, and the ambient stability was nearly neutral. In contrast, accidental releases are likely to involve time-variable source emissions over rough surfaces including obstacles such as buildings, tanks, and pipes, typical of an industrial facility, and can occur during any type of meteorological scenario. Evaluations of commonly used dense gas dispersion models with limited existing field and wind tunnel data suggest that they are biased (by as much

\* Corresponding author. Tel.: +1-703-993-1992; fax: +1-703-993-1980.

E-mail address: shanna@gmu.edu (S.R. Hanna).

as a factor of two to four) for transient releases (Hanna et al., 1993; Hanna and Chang, 1995).

The comprehensive PERF 93-16 atmospheric dispersion modeling study also included wind tunnel experiments (see Briggs et al., 2001). The overall PERF 93-16 data analysis and model development activities have been designed to improve our knowledge of six primary technical issues: the rate of vertical entrainment into dense gas clouds, the along-wind dispersion coefficient  $\sigma_x$ , the cloud advection speed  $u_e$ , the effects of surface roughness  $z_0$ , the effects of atmospheric stability, and the effects of obstacles.

Because a key parameter in the modeling of all of these technical components is the ambient atmospheric boundary layer friction velocity,  $u^*$ , the Kit Fox experiments and the wind tunnel experiments placed a priority on the accurate determination of  $u^*$ . As an example of the importance of  $u^*$ , the entrainment of ambient air into ground-based dense gas clouds is parameterized by assuming that the vertical entrainment velocity,  $w_e$ , is proportional to the ambient friction velocity,  $u^*$ , and is a function of the cloud Richardson number,  $Ri^*$ :

$$Ri^* = g(\rho_p - \rho_a)h/\rho_a u^{*2}, \quad (1)$$

where  $g$  is the acceleration of gravity,  $h$  is the local cloud depth,  $\rho_p$  is local cloud density, and  $\rho_a$  is ambient density. Briggs et al. (2001) analyzed data from three wind tunnels and found that, for  $Ri^*$  up to 20, the observations showed reasonable agreement with the following relation:

$$w_e = 0.65u^*/(1.0 + 0.2Ri^*). \quad (2)$$

This revised entrainment equation was substituted for the existing entrainment equation in a widely used dense gas dispersion model (HEGADAS, Witlox, 1994) and the revised and existing entrainment options evaluated with the Kit Fox field observations.

Besides the entrainment equation, other algorithms in dense gas dispersion models make use of  $u^*$ . For example, the cloud advective speed,  $u_e$ , and the along-wind dispersion coefficient,  $\sigma_x$ , are each proportional to  $u^*$ . Because  $u^*$  can be determined from an observation of the wind speed near the ground and from an estimate of the surface roughness length,  $z_0$ , it is therefore important to be able to estimate  $z_0$  and the effects of variations in  $z_0$ . The Kit Fox experiments allowed testing of the model parameterizations over two different sets of surface roughness elements, with  $z_0$  varying by an order of magnitude.

The following sections describe the Kit Fox field experiment, present the results of analysis of some of the observations, and suggest whether existing algorithms in dense gas dispersion models agree with these observations.

A specific dense gas dispersion model, HEGADAS, described by Witlox (1994) and Post (1994) was evaluated

with the Kit Fox data. In this paper, Version 3.0 of the model (the so-called “original” model version) is compared with Version 3 + (the so-called “revised” model version described by Hanna and Chang, 1995), which contains two primary modifications involving the along-wind dispersion and the cloud advection speed.

## 2. Kit Fox field experiment design

The Kit Fox dense gas field experiment was conducted in August and September, 1995, at the Frenchman Flat area of the Nevada Test Site. The field operations were carried out by Desert Research Institute (DRI) and Western Research Institute (WRI, 1998). Dense gas ( $\text{CO}_2$ ) was released from a ground-level  $1.5 \text{ m} \times 1.5 \text{ m}$  area source. The entire experimental setup was intended to represent an industrial site at about 1/10 of full scale, for it was impractical to carry out the experiment at an actual oil refinery or chemical plant, and it would have been prohibitively expensive to construct an artificial full-scale refinery at the test site. To simulate an oil refinery or chemical plant at about 1/10 scale, the flat desert lake bed at Frenchman Flat had thousands of flat billboard-shaped roughness elements installed over a  $120 \text{ m} \times 314 \text{ m}$  area in order to increase the roughness to a value that was about 1/10 of the value typical of an industrial site and its surroundings (see Fig. 1 for a plot plan of the experiment, showing locations of the roughness elements and the instruments). The roughness arrays, which were constructed of rectangular sections of plywood placed on the sand perpendicular to the mean flow direction, were designed by wind tunnel experiments (Petersen and Cochran, 1995; Snyder, 1995). The final

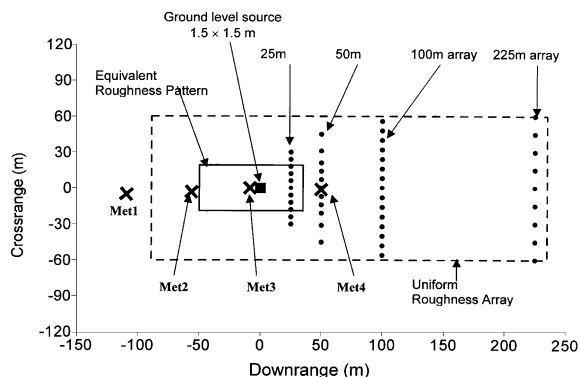


Fig. 1. Plot plan of the Kit Fox site showing the locations of the meteorological towers, the concentration monitoring arcs, the source, the ERP array, and the URA array. The EPA meteorological tower is off the figure at a location given by Downrange = -102 m and Crossrange = -177 m. The figure is adapted from WRI (1998).

design represents the maximum efficiency in generating roughness for the least number of plywood obstacles. The Kit Fox field experiment was characterized by the following geometric setup, gas release methodology, gas concentration observations, and meteorological observations.

- The taller Equivalent Roughness Pattern (ERP) (2.4 m square plywood billboards) roughness array was installed on the inner 39 m × 85 m (cross-wind × along-wind) rectangle, with the dense gas source near the center. The boundaries of the ERP array are shown by the solid rectangle in Fig. 1. The roughness elements were staggered, with 6.1 m lateral spacing and 8.1 m along-wind spacing. Observations of wind profiles suggested that the roughness length,  $z_0$ , of the ERP was about 0.12–0.24 m.
- The shorter Uniform Roughness Array (URA) (0.2 m high × 0.8 m wide rectangular plywood billboards) was installed on the outer 120 m × 314 m (cross-wind × along-wind) rectangle. The boundaries of the URA array are shown by the dashed rectangle in Fig. 1. The URA roughness elements were also staggered, with 2.4 m lateral spacing and 2.4 m longitudinal spacing. Observations of wind profiles suggested that the roughness length,  $z_0$ , of the URA was about 0.01–0.02 m.
- Eighty-four fast-response (one reading per second) concentration monitors were installed on the four downwind arcs (25, 50, 100, and 225 m) shown in Fig. 1. Some concentration monitors were mounted on 5–10 m towers, where there were three towers on each of the 25, 50, and 100 m arcs.
- Meteorological instruments (including 10 sonic anemometers) were installed on five towers (see Fig. 1) with heights 24 m (EPA), 4.9 m (Met1), 8 m (Met2), 4.9 m (Met3), and 8 m (Met4).
- CO<sub>2</sub> was released from a 1.5 m × 1.5 m area source near the middle of the ERP, with a nearly constant emission rate of about 4 kg s<sup>-1</sup> for 2–5 min (continuous “plumes”) and 20 s (finite duration “puff”) periods when the ERP was in place.
- When the ERP was removed (leaving the URA), the CO<sub>2</sub> release rate was decreased to about 1.6 kg s<sup>-1</sup>. There were 13 puff and 6 continuous plume trials in the ERP experiments, and 21 puff and 12 continuous plume trials in the URA experiments.
- Schedule: One week of field tests (trials 2–5) took place with the ERP and the URA roughness obstacles installed. One week of field tests (trials 6–8) took place with only the URA roughness obstacles in place. These two weeks of experiments comprise the core of the Kit Fox experiments. One week of the so-called EPA field tests then took place with the URA and ERP roughness obstacles removed (i.e., flat desert). This paper describes the PERF Kit Fox experiments (with the ERP and URA roughness arrays), and a separate EPA

report (Coulombe et al., 1999) describes the EPA flat desert experiments. Most of the analysis in this paper concerns the Kit Fox ERP and URA field trials, and the EPA field trials are included only in the analysis of maximum concentrations in Section 3.2.3.

The HEGADAS 3.0 dense gas dispersion model (Witlox, 1994; Post, 1994) was used to help design the placement ( $x$ ,  $y$ , and  $z$ ) of concentration monitors and meteorological instruments in the Kit Fox field experiment. The model predictions were also used to plan the source release rates, so that the desired dense gas effects (primarily determined by  $Ri^*$ , as shown by Eqs. (1) and (2)) could be detected with minimal CO<sub>2</sub> gas releases. Model predictions of concentrations, cloud height, and cloud width were generated for a variety of source conditions, meteorological inputs, and surface roughnesses, in order to plan the calibration ranges for the instruments and their locations in  $x$ ,  $y$ , and  $z$ . The lateral spacings of the concentration monitors (about 6 m on the closest arc and about 10 m on the farthest arc) and their maximum heights (about 5 m on the closest arc and about 10 m on the farthest arc) on the nine towers were expected to capture the cloud, according to these model calculations.

### 3. Characteristics of 52 trials available from Kit Fox experiment

There were 52 independent Kit Fox data trials, with about 2/3 for “puff” or “finite duration” 20 s releases, and about 1/3 for “continuous plume” 120–450 s releases. A summary of the major characteristics of each of the 52 tests is given in Table 1, including the time duration,  $T_d$ , of the release, the date and start time (PDT or local daylight savings time), the source emission rate,  $Q$ , the wind speed,  $u$ , at 2 m elevation on the EPA tower and on the Met4 tower, the wind direction, WD, at 2 m elevation on the Met4 tower, and the derived friction velocity,  $u^*$ , and Monin–Obukhov length,  $L$ , from the Met3 or Met4 tower. The locations of the meteorological towers are shown in Fig. 1. Table 1 also contains comments concerning whether the cloud was observed to be on the edge of the monitoring arcs or had other distinguishing characteristics.

#### 3.1. Analysis of meteorological observations

The wind speeds from the EPA tower are listed in Table 1 because those observations represent conditions over the flat desert outside of the Kit Fox roughness arrays. The roughness length,  $z_0$ , of the flat desert is about 0.0002 m, while the roughness length for the ERP and URA arrays is about 0.12–0.24 m and about 0.01–0.02 m, respectively. The observations on the Met4 tower are listed and are used in most of the theoretical

Table 1

Summary of 52 Kit Fox trials, including duration of release ( $T_d$ ), date and start time, source emission rate ( $Q$ ), wind speed at the 2 m level on the EPA and Met4 towers, wind direction at the 2 m level on the Met4 tower, friction velocity ( $u^*$ ) and Monin–Obukhov length ( $L$ ) at the Met4 tower, and comments concerning the location of the observed cloud

Trial	$T_d$ (s)	Date	Start time PDT	$Q$ ( $\text{kg s}^{-1}$ )	$u$ ( $\text{m s}^{-1}$ )	$u$ ( $\text{m s}^{-1}$ )	WD(deg) Met4 2 m	$u^*$ ( $\text{m s}^{-1}$ )	$L$ (m)	Comments
					EPA 2 m	Met4 2 m		Met3 or 4	Met3 or 4	
2-1	25	24 Aug	18:14:00	4.28	6.90	3.00	217	0.42	140	On L edge
2-6	360	24 Aug	19:35:02	3.89	3.36	2.46	199	0.21	17	On L edge
3-1	20	25 Aug	18:23:40	4.09	5.80	2.07	216	0.4	130	
3-2	20	25 Aug	18:35:12	4.30	6.30	2.22	236	0.42	140	
3-3	20	25 Aug	18:50:53	3.80	5.90	2.02	232	0.4	130	
3-4	20	25 Aug	19:05:48	3.75	3.85	1.55	230	0.31	35	
3-5	300	25 Aug	19:10:47	3.99	3.09	1.40	240	0.22	19	On R edge
3-6	20	25 Aug	19:24:24	3.76	2.85	1.06	246	0.21	17	
3-7	20	25 Aug	19:28:28	3.65	2.70	1.10	233	0.21	17	
4-3	20	26 Aug	19:29:11	3.90	2.41	1.29	214	0.11	4	On L edge
4-4	450	26 Aug	19:33:40	3.89	2.11	0.79	225	0.067	2	Smooth Dist.
5-1	20	28 Aug	19:27:04	4.00	7.10	3.01	225	0.42	140	
5-2	20	28 Aug	19:43:45	4.03	5.50	2.27	220	0.42	140	
5-3	120	28 Aug	19:50:16	3.92	5.30	2.55	222	0.4	130	
5-4	120	28 Aug	19:56:06	3.70	4.60	2.14	224	0.34	80	
5-5	20	28 Aug	20:01:11	3.76	4.80	2.08	220	0.37	100	
5-6	20	28 Aug	20:18:11	3.74	3.90	1.37	229	0.24	33	
5-7	20	28 Aug	20:25:17	3.98	3.05	1.44	234	0.21	17	
5-8	180	28 Aug	20:29:11	3.77	2.71	1.26	241	0.17	8	On R edge
6-1	20	29 Aug	18:30:18	1.28	5.80	4.16	227	0.32	80	
6-2	20	29 Aug	18:35:31	1.65	5.90	3.69	211	0.34	80	
6-3	20	29 Aug	18:38:06	1.71	4.50	3.44	230	0.29	50	
6-4	120	29 Aug	18:43:45	1.76	5.80	3.86	235	0.34	80	
6-5	120	29 Aug	18:59:37	1.88	3.88	3.05	233	0.25	36	
6-6	180	29 Aug	19:05:32	2.07	2.83	2.17	234	0.19	19	
6-7	20	29 Aug	19:13:07	1.79	2.68	1.86	236	0.13	6	
6-8	20	29 Aug	19:16:56	1.64	2.86	1.61	235	0.12	5	
6-9	300	29 Aug	19:22:10	1.47	2.33	1.90	238	0.12	5	
7-2	140	30 Aug	18:11:51	1.91	4.46	3.80	229	0.31	35	
7-3	180	30 Aug	18:25:37	1.65	4.16	3.10	228	0.23	18	
7-4	20	30 Aug	18:30:42	1.68	3.20	1.95	234	0.21	14	
7-5	180	30 Aug	18:36:15	1.73	3.91	2.75	228	0.21	17	
7-6	20	30 Aug	18:54:12	1.49	3.37	2.60	231	0.21	21	Low C Arc 1
7-8	20	30 Aug	19:09:32	1.64	3.26	2.46	222	0.19	8.8	
7-9	180	30 Aug	19:12:57	1.72	2.82	2.16	224	0.16	5.9	
7-10	20	30 Aug	19:19:08	1.70	2.42	1.98	229	0.13	4.2	
7-11	20	30 Aug	19:24:17	1.63	2.55	1.91	234	0.13	6.1	
7-12	255	30 Aug	19:27:23	1.54	2.00	1.84	242	0.1	3.4	Merges with 7-13
7-13	20	30 Aug	19:34:08	1.30	1.83	1.29	227	0.08	2.1	
7-14	20	30 Aug	19:41:48	1.41	1.81	1.38	246	0.06	1.5	Late at Arc 4
8-1	20	31 Aug	18:22:06	1.11	5.81	4.29	223	0.35	190	
8-2	20	31 Aug	18:28:01	1.62	6.20	4.18	239	0.34	76	R edge Arc 4
8-3	20	31 Aug	18:31:54	1.62	5.92	3.55	233	0.34	80	
8-4	20	31 Aug	18:46:21	1.65	5.10	3.08	242	0.32	99	R edge Arc 4
8-5	150	31 Aug	18:53:30	1.51	4.64	3.97	238	0.32	68	R edge Arc 4
8-6	20	31 Aug	19:03:40	1.59	4.54	3.45	239	0.27	35	
8-7	20	31 Aug	19:07:06	1.76	5.35	3.03	234	0.27	36	
8-8	120	31 Aug	19:12:00	1.62	4.72	3.80	236	0.27	39	
8-9	20	31 Aug	19:20:06	1.57	3.80	2.54	226	0.24	33	
8-10	20	31 Aug	19:34:46	1.58	3.30	2.11	236	0.2	20	
8-11	240	31 Aug	19:58:22	1.50	3.24	2.34	241	0.19	19	
8-12	20	31 Aug	20:08:02	1.46	2.86	2.37	246	0.18	17	R edge Arc 4

analyses and for inputs to models because that tower is located on the concentration monitoring arc 2 ( $x = 50$  m) in the middle of the roughness array and in the middle of the cloud as it is transported downwind. That tower is in the URA roughness array, 50 m downwind of the source and 15 m downwind of the edge of the ERP array (when the ERP array is in place for trials 2–5). For the ERP/URA roughness arrays (trials 2–5), the table shows that the Met4 wind speeds are less than 50% of the EPA tower wind speeds. For the URA roughness arrays (trials 6–8), the Met4 wind speeds are about 70% of the EPA tower wind speeds.

The wind speed data from the four Met towers and from the EPA tower primarily reflect the local underlying surface roughness. As Goode and Belcher (1999) state, when there is an array of alternating heterogeneous surface roughnesses, the wind speeds below a certain “blending” height will reflect the local surface, whereas the wind above this “blending” height will reflect the integrated effect of the varying surfaces. The “blending” height is found to approximately equal about 20% of the width of the roughness sections, for regular variations in roughness. However, the Kit Fox site consisted of only single groups of surface roughness types (e.g., the ERP and the URA), whereas Goode and Belcher (1999) were concerned with areas with alternating roughness areas such as farm fields with forested areas between each field.

When available, the sonic anemometer observations on the Met3 or Met4 tower are used for estimating  $u^*$  and  $L$  in Table 1, where  $u^* = \sigma_w/1.3$  and  $w'T' = 0.2\sigma_w\sigma_T$ . Then  $L = (u^{*3}/0.4)/((g/T)w'T') = (\sigma_w^2/0.136)/((g/T)\sigma_T)$ . For URA trials 7 and 8,  $u^*$  and  $L$  estimates are based on observations on the Met3 tower (no sonic anemometer data are available for the Met4 tower). Because no sonic anemometer data are available from either the Met3 or Met4 tower in trial 6, the estimates of  $u^*$  and  $L$  for trial 6 are based on extrapolations from the observations on the Met1 tower using empirical relations found between the data from the Met1 and Met3 towers for trials 7 and 8. For the ERP trials, where no sonic anemometer data were available from the Met3 and Met4 towers,  $u^*$  and  $L$  are based on extrapolations from the observations on the Met1 tower (the mean wind profile observations from the Met1 and Met3 towers suggest that  $u^*(\text{Met4})/u^*(\text{Met1}) = 1.75$ ).

An alternate way to estimate  $u^*$  and  $L$  is to attempt to fit observed vertical profiles of wind speed and temperature on the same tower using least-squares regression procedures and standard log-linear profile formulas. The surface roughness lengths,  $z_0$ , listed above were assumed to equal the values determined by a comprehensive analysis of all profiles at the site. The  $u^*$  and  $L$  values derived from the sonic anemometers were checked against the values derived from the profiles in order to determine if there was any bias. It was found that the mean bias was small although the scatter was about a factor of two.

It is important to note that the assumption is being made that changes of wind speed, heat flux, turbulence, and  $u^*$  within the dense gas cloud do not need to be accounted for directly. It is assumed that it is sufficient to know the values of winds, turbulence,  $u^*$ , and heat flux in the ambient air. There is no assurance a priori whether this assumption will be useful, but it has been made successfully in many earlier dense gas field studies and modeling exercises.

### 3.2. Analysis of dense gas cloud concentration observations

The 1 s  $\text{CO}_2$  concentration observations from the monitors on the four monitoring arcs ( $x = 25, 50, 100,$  and  $225$  m) shown in Fig. 1 were plotted and analyzed for each of the 52 trials. This exercise was carried out in order to gain an understanding of the behavior of the data prior to testing the HEGADAS dense gas dispersion model. The master data set (WRI, 1998), was used to generate time-integrated concentrations,  $C_t$ , for each monitor for each of the 52 trials in Table 1, and to generate cross-wind-integrated near-ground concentrations,  $C_y$ , for each monitoring arc for each second of each trial.

#### 3.2.1. Along-wind cloud dimensions

The  $C_y$  time series were used to estimate several key times that are important to understanding the physics of dense gas dispersion and developing and evaluating models. These observations include, for example, the times (since initial release) at each monitoring arc for the cloud to arrive, for the cloud to depart, for the  $0.5C_{y\text{max}}$  arrival and departure, for the  $0.1C_{y\text{max}}$  arrival and departure, for the peak 1 s  $C_{y\text{max}}$ , and for the peak 20 s  $C_{y\text{max}}$ . Note that  $C_{y\text{max}}$  is the maximum  $C_y$  observation for each individual time series. Estimates were made of the cloud speed,  $u_c$ , which is assumed to equal the arc distance divided by the travel time to  $0.5C_{y\text{max}}$ . The time interval between the arrival and departure of  $0.5C_{y\text{max}}$ , known as  $dt(0.5)$ , and the time interval between the arrival and departure of  $0.1C_{y\text{max}}$ , known as  $dt(0.1)$ , were used to estimate the standard deviation  $\sigma_t = 0.212dt(0.5) + 0.117dt(0.1)$ , where the constants, 0.212 and 0.117, are valid for a Gaussian distribution. The along-wind dispersion coefficient,  $\sigma_x$ , was assumed to equal  $u_c\sigma_t$ . The Kit Fox data suggest that  $\sigma_x = 2u^*t$ , which agrees with a recent similarity model proposed by Hanna and Franzese (2000).

#### 3.2.2. Vertical and lateral cloud dimensions

The  $y$ - $z$  cross sections of time-integrated concentrations,  $C_t$ , were used to estimate the vertical cloud height,  $h(0.5)$ , and the lateral cloud standard deviation,  $\sigma_y$ , for each test. The vertical cloud height,  $h(0.5)$ , was estimated as the height where the concentration,  $C_t$ , decreased to 0.5 times its maximum near-ground-level concentration.

As was done for  $\sigma_x$ , the lateral  $\sigma_y$  was estimated from  $d_y(0.1)$  and  $d_y(0.5)$ , defined as the lateral distances between the points on either edge of the plume where the concentrations of  $0.5C_{t\max}$  and  $0.1C_{t\max}$  were found. Then  $\sigma_y = 0.212d_y(0.5) + 0.117d_y(0.1)$ . If both sides of the lateral concentration distribution were not fully captured on the monitoring arc, the observed  $\sigma_y$  was estimated from the data available on one side of the plume.

The cloud  $h(0.5)$  and  $\sigma_y$  estimates from each of the 52 trials and the four monitoring arcs have been analyzed in order to determine if some general conclusions could be reached. For the clouds being transported over the 0.20m URA roughness elements, the  $\sigma_y$  observations were found to be several times larger than the  $h(0.5)$  observations, with the largest differences (over an order of magnitude) found to occur for low-wind ambient conditions, as expected for dense gas clouds. The  $h(0.5)$  values at the 25 m arc over the URA ranged from 0.7 m for low winds to 1.5 m for high winds. Note that the  $h(0.5)$  observations were always 3.5 or more times the height of the URA obstacles (0.2 m). In contrast, the  $h(0.5)$  values over the 2.4 m ERP roughness elements at the 25 m monitoring arc were always approximately equal to the obstacle height (2.4 m), or a little higher (3 or 4 m). Evidently, the turbulence in the recirculating cavities behind the ERP obstacles caused the dense gas cloud to be mixed vertically to approximately the height,  $H_r$ , of the obstacles. As will be seen later, it is difficult for current dense gas models to properly simulate this wake-mixing phenomenon. Nevertheless, it is clear that the Kit Fox URA experiments were characterized by cloud heights,  $h(0.5)$ , greater than or equal to the obstacle heights.

The cloud height,  $h(0.5)$ , observations for the ERP roughness elements suggest very little dependence on wind speed. The  $h(0.5)$  values were observed to equal about 3, 5.5, and 6.5 m on the 25, 50, and 100 m downwind arcs, respectively. On the other hand, the  $h(0.5)$  observations for the URA roughness elements showed about a factor of two decrease at all downwind distances as the wind speed decreases from "high" to "low".

The observed lateral cloud standard deviations,  $\sigma_y$ , approximately doubled or tripled as distance increased

from 25 to 225 m. As is the case with  $h(0.5)$ , there was more variation of  $\sigma_y$  with wind speed for the URA array (factor of two or three) than for the ERP array (less than a factor of two). The variation of  $\sigma_y$  with distance was not expected to be closely related to the known variation for passive gas (neutrally buoyant) clouds, since the dense gas clouds had a larger initial lateral spread due to gravity effects.

The discussions above for the ERP array should also recognize that only the 25 m monitoring arc was within the ERP ( $H_r = 2.4$  m) obstacles. The 50 m arc was within the URA ( $H_r = 0.2$  m) obstacles, about 15 m downwind of the boundary between the ERP and the URA. The 100 and 225 m arcs were well within the URA. However, meteorological observations showed that, after leaving the ERP, the boundary layer took several tens of meters to readjust to being over the URA. As stated earlier, studies such as that by Goode and Belcher (1999) provide criteria for the depth of the layer affected by a new roughness surface as a function of downwind distance. Typically this internal boundary layer has a slope of about 20% with downwind distance. As a consequence, the lateral dispersion observations at the 50, 100, and 225 m arcs were influenced by a transient boundary layer that was responding to both the ERP and URA roughnesses.

### 3.2.3. Cloud travel speeds $u_c$

Cloud travel speeds,  $u_c$ , were estimated for all Kit Fox trials and arcs. These speeds were assumed to equal monitoring arc distance divided by time of travel, and thus represent the average speed over the cloud's travel from the source to that arc. This definition is different from that used in the software of most models, where  $u_c$  is defined as the local cloud travel speed (at the point where the concentration measurements are made). However, this latter local definition could not be calculated from the available observations. It should also be noted that the  $u_c$  values analyzed in this section were based on the observed times when the cloud cross-wind-summed concentration,  $C_y$ , first rose to 50% of its maximum value. The plots of observed  $u_c$  versus observed wind speed for

Table 2

Summary of median observed cloud advection speeds,  $u_c$ , divided by  $u_{Met4}$  (2 m) and  $u_{EPA}$  (2 m) on the four downwind arcs for the four classes of release durations and roughness arrays

	$u_c/u_{Met4}(2\text{ m})$				$u_c/u_{EPA}(2\text{ m})$			
	25 m	50 m	100 m	225 m	25 m	50 m	100 m	225 m
ERP puff	0.3	0.6	0.8	1.0	0.15	0.25	0.32	0.5
ERP continuous	0.25	0.4	0.6	0.9	0.1	0.16	0.25	0.4
URA puff	0.3	0.4	0.55	0.75	0.2	0.3	0.35	0.5
URA continuous	0.2	0.3	0.4	0.6	0.15	0.25	0.3	0.4

the four monitoring arcs for the four source release classes (ERP puffs, ERP continuous plumes, URA puffs, and URA continuous plumes) were used to develop the summary in Table 2, where ratios of  $u_e/u(2\text{ m})$  are given for observations on the Met4 tower (on the 50 m arc) and on the EPA tower (in the flat desert). The cloud was observed to accelerate, with speeds increasing by about a factor of three or four, as it moves downwind from the 25 m arc to the 225 m arc. The increase in cloud travel speed,  $u_e$ , as distance increased was primarily caused by the vertical dispersion of the cloud, which brought it under the influence of higher wind speeds at higher levels. The effects of cloud density may also have influenced this variation.

As suggested by Hanna and Chang (1995) and as will be seen in Section 4, the peak concentrations for the puffs were sensitive to the cloud advection speed,  $u_e$ . The faster the puff moves, the less time it has to disperse before it arrives at a given monitoring arc. Thus, for all other conditions constant, puff peak concentrations will increase as the puff advection speed increases, as suggested by Britter and McQuaid (1988).

#### 3.2.4. Variation of maximum normalized concentrations as $z_0$ changes (ERP, URA, and EPA)

The increased turbulence intensity over the ERP and URA roughness obstacles should have led to increased turbulent dispersion and hence a tendency towards reduced maximum ground-level concentrations from a given ground-level source release, all conditions being the same (i.e., constant net radiation and constant free-stream wind speed). This hypothesis is valid at heights within the atmospheric boundary layer such that the boundary layer has adjusted to the combined effects of individual roughness obstacles. The reduction in maximum ground-level concentration with an increase in surface roughness length could be clearly seen in the Kit Fox experiments, which were characterized by cloud heights,  $h(0.5)$ , always greater than the obstacle height at the monitoring arcs. In addition, the data from the EPA flat desert tests (Coulombe et al., 1999), conducted in the week following the ERP/URA and URA tests, could also be used in the analysis. The roughness lengths for the three sets of trials were about 0.12 m for the ERP/URA trials, 0.01 m for the URA trials, and 0.0002 m for the EPA trials. The source emission rate for the EPA flat desert trials was about  $1.5\text{ kg s}^{-1}$ , as for the URA. The source emission rate was about  $4\text{ kg s}^{-1}$ , for the ERP/URA trials.

Concentration data were analyzed from the 50, 100, and 225 m arcs, since the 25 m arc was not used for the flat desert EPA trials. The maximum observed normalized concentration,  $(C/Q)_{\text{max}}$ , at the monitors closest to the ground at a given downwind distance was chosen from all the trials for each roughness group (i.e., ERP/URA, URA, and EPA flat desert) and each release

type (i.e., continuous plume or puff). For the continuous plumes, it was appropriate to normalize by the mass emission rate ( $Q_{\text{rate}}$ , in  $\text{kg s}^{-1}$ ), while for the puffs, it was appropriate to normalize by the total mass emission ( $Q_{\text{tot}}$ , in kg) over the 20 s release period.

For the continuous releases, the maximum normalized ground-level concentrations,  $(C/Q_{\text{rate}})_{\text{max}}$ , for the three roughnesses occurred during similar meteorological conditions, with light winds of about  $2\text{ m s}^{-1}$ . This result agrees with our expectations for continuous plumes. For the puff releases, the maximum normalized ground-level concentrations,  $(C/Q_{\text{tot}})_{\text{max}}$ , occurred for wind speeds averaging  $3.2\text{ m s}^{-1}$  for the URA trials and  $5.5\text{ m s}^{-1}$  for the ERP/URA trials, agreeing with the conclusion of Britter and McQuaid (1988). However, for the EPA flat terrain puff releases, the maximum normalized concentration,  $(C/Q_{\text{tot}})_{\text{max}}$ , occurred for light winds of about  $2\text{ m s}^{-1}$ , suggesting that the cloud density effects outweighed the dilution time effects for the EPA flat terrain tests. The vertical entrainment rate into a dense gas cloud is a strong function of ambient turbulence, which was minimized over the flat terrain.

Much higher maximum normalized ground-level concentrations (i.e.,  $(C/Q)_{\text{max}}$ ) were consistently observed for the experiments with the smaller surface roughnesses, for all three monitoring arcs and for both continuous plume and puff releases. There was a steady increase in  $(C/Q)_{\text{max}}$  as roughness decreased from ERP ( $z_0 = 0.1$  or  $0.2\text{ m}$ ) to URA ( $z_0 = 0.01$  or  $0.02\text{ m}$ ) to flat desert ( $z_0 = 0.0002\text{ m}$ ). The presence of the URA roughness obstacles (height 0.2 m) caused increased dilutions of about a factor of five when compared with the flat terrain observations. The presence of the ERP roughness obstacles (height 2.4 m) caused even larger increased dilutions of about a factor of 20 when compared with the flat terrain observations. These data support a  $(C/Q)_{\text{max}} \propto z_0^{-1/2}$  relation, with the  $-1/2$  power law consistently found for both puff and plume releases. Most of the commonly used dense gas dispersion models should be able to simulate this effect, since most models require input of surface roughness length,  $z_0$ , which will result in larger predictions of turbulence intensity and therefore lower predictions of concentrations over rougher surfaces.

It should be emphasized that these results, concerning the effects of surface roughness on  $(C/Q)_{\text{max}}$ , are most valid for clouds with heights,  $h(0.5)$ , greater than the obstacle heights,  $H_r$ , and for downwind fetches of at least  $10H_r$ , over the new roughness surface, thus assuring that the boundary layer is in equilibrium with the underlying roughness obstacles. As Macdonald et al. (1997) and Davidson et al. (1995) have shown, when the obstacles are closely packed and when  $h \ll H_r$ , the peak concentration may not decrease significantly as surface roughness increases, due to relatively large reductions in wind speed deep within the roughness obstacles. In these cases, the maximum concentration may either increase or decrease

as roughness length increases, depending on which of the following effects is dominant – the increased turbulence intensity or the decreased wind speed.

#### 4. Evaluations of a dense gas dispersion model (HEGADAS 3) with Kit Fox data

##### 4.1. Description of evaluation process

As part of the PERF 93-16 atmospheric dispersion modeling research project (Hanna and Steinberg, 2001), the Kit Fox field data were used to evaluate dense gas dispersion models. We chose to emphasize the HEGADAS 3.0 model (Witlox, 1994; Post, 1994) and the revised HEGADAS 3+ model (Hanna and Chang, 1995), and included sensitivity studies using alternate algorithms suggested by analysis of the data. Earlier in the research project, Hanna and Chang (1995) had modified HEGADAS 3.0 based on wind tunnel observations made by Petersen (1992) of short-duration dense gas clouds which were dispersing, in a neutral ambient boundary layer, over rough surfaces typical of chemical plants or refineries. The wind tunnel observations had suggested that the HEGADAS 3.0 model was overpredicting by a factor of four to eight, with the largest overpredictions for the releases with the shortest durations. Hanna and Chang (1995) proposed and tested a revised version of the code, HEGADAS 3+, which contained modifications to two major components: (1) the along-wind dispersion coefficient,  $\sigma_x$ , was increased by a factor of two, and (2) the advection speed,  $u_e$ , of the cloud was decreased by 30%. The revised HEGADAS 3+ model was shown by Hanna and Chang (1995) to agree well with the Petersen (1992) wind tunnel observations, and in the current study has been evaluated independently with the Kit Fox field data.

These evaluations make use of the transient version of the model, HEGADAS-T (Witlox, 1994). There is also a steady-state version, HEGADAS-S, which is similar to HEGADAS-T but has not been the focus of the current evaluations.

The statistical evaluation methodology is similar to that used by Hanna et al. (1993). Fundamental performance measures include the geometric mean, MG; the geometric variance, VG; the fractional bias, FB; the normalized mean square error, NMSE, and the fraction of  $C_p$  within a factor of two of  $C_o$ , FAC2:

$$MG = \exp(\overline{\ln(C_o/C_p)}), \quad (3)$$

$$VG = \exp(\overline{(\ln(C_o/C_p))^2}), \quad (4)$$

$$FB = 2(\overline{C_o} - \overline{C_p})/(\overline{C_p} + \overline{C_o}), \quad (5)$$

$$NMSE = \overline{(C_o - C_p)^2}/\overline{C_o C_p}, \quad (6)$$

$$FAC2 = \text{fraction of } C_p \text{ within a factor of two of } C_o, \quad (7)$$

where subscripts o and p indicate observed and predicted concentrations. The concentration,  $C$ , is the maximum concentration observed or predicted on a given monitoring arc distance. The performance measures MG and FB both measure relative mean bias, where MG is based on  $(\ln C)$  and FB is based on  $C$ . Similarly, the performance measures VG and NMSE both measure relative scatter, where VG is based on  $(\ln C)$  and NMSE is based on  $C$ . Comparisons of predicted and observed variables such as  $u_e$ ,  $h(0.5)$ ,  $\sigma_y$ , and  $\sigma_z$  are also made using the above definitions of FB, NMSE, and FAC2, but with the appropriate variable (e.g.,  $\sigma_y$ ) substituted for the concentration  $C$  in Eqs. (5)–(7).

The evaluation methodology also includes plots of model residual trends (i.e.,  $C_p/C_o$  versus independent variables such as  $x$ ,  $u$ ,  $u^*$ , and  $L$ ). Comparisons are also presented of predicted and observed highest concentrations for each category (e.g., ERP puffs).

The first step in the model evaluation exercise involved the evaluations of 25 HEGADAS sensitivity runs using various combinations of possible model inputs and algorithms. The inputs that were tested included the  $u^*$  and  $L$  scaling parameters, the roughness length  $z_0$ , the reference height for wind observations, the factor increase in  $\sigma_x$  and  $u_e$ , the vertical entrainment coefficient, and off-site (EPA tower) versus on-site (Met4 tower) winds. Specific choices concerning inputs were based on (1) the parameterizations in HEGADAS 3.0 and HEGADAS 3+, and (2) alternate parameterizations based on analysis of the Kit Fox concentration and meteorological observations (e.g., see Section 3). The results of the evaluations of the 25 sensitivity runs were thoroughly discussed in the project report (Hanna et al., 1999) and were summarized in a separate paper (Hanna and Chang, 1999). In most cases, only minor sensitivities were found. For example, the new entrainment equation (2) was found to not produce a significant improvement over the old equation. A slight improvement in HEGADAS 3+ performance was found with a version which used “two roughnesses”. In that version, for the ERP/URA trials, the model was run separately with  $z_0 = 0.12$  m (the ERP value) for the 25 and 50 m arcs, and with  $z_0 = 0.035$  m (the geometric mean of the ERP and URA  $z_0$  values) for the 100 and 225 m arcs. Consequently, the final evaluations, reported in the next section, are given for the three model versions denoted as HEGADAS 3+, HEGADAS 3.0, and HEGADAS 3+ (two roughnesses).

##### 4.2. Evaluation results for HEGADAS 3+, HEGADAS 3.0, and HEGADAS 3+ (two roughnesses)

The model evaluation methodology described in the previous section was used to evaluate the predictions of the HEGADAS 3+, HEGADAS 3.0, and HEGADAS 3+ (two roughnesses) models with the Kit Fox data. Fig. 2 contains a plot of the overall MG versus VG for



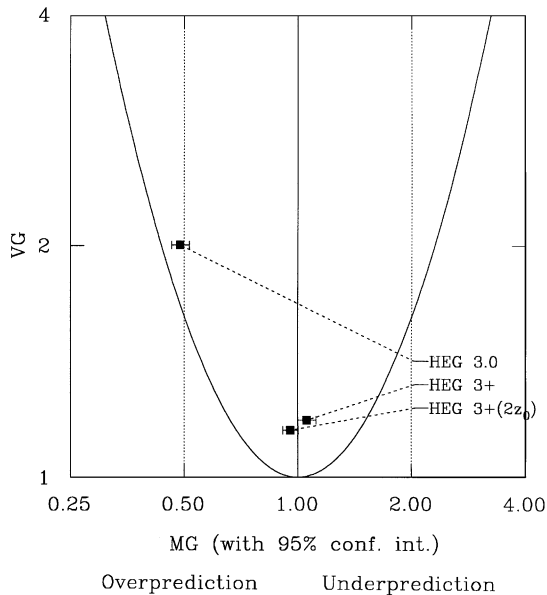


Fig. 2. Plot of geometric mean (MG) versus geometric variance (VG) for the Kit Fox data for the three model runs, HEGADAS 3 +, HEGADAS 3.0, and HEGADAS 3 + (two roughnesses). A model with  $MG = VG = 1.0$  is a perfect model. The vertical dotted lines at  $MG = 0.5$  and  $2.0$  represent a factor of two overprediction and underprediction. The lateral bars for each model represent 95% confidence intervals on MG. The parabola represents the minimum VG for each MG due to systematic bias.

the three models for a concentration averaging time of 1 s. The figure demonstrates that the overall geometric mean, MG, is close to unity (i.e., mean bias less than 10%) for the HEGADAS 3 + model and for the HEGADAS 3 + (two roughnesses) model, while the MG for the original HEGADAS 3.0 model is 0.5 (i.e., there is a factor of two overprediction of the mean concentrations). Note that in this figure a perfect model would be represented by a point at  $MG = VG = 1.0$ . The geometric variance, VG, is about 1.15 or 1.20 for the HEGADAS 3 + model and for the HEGADAS 3 + (two roughnesses) model (i.e., relative scatter of about 30 or 40%), while the VG for the original HEGADAS 3.0 model is about 2 (i.e., relative scatter of about a factor of 2.2). Thus the points for the HEGADAS 3 + model and for the HEGADAS 3 + (two roughnesses) model are very close in Fig. 2, while the point for the original HEGADAS 3.0 model is an outlier.

Residual plots (i.e.,  $C_p/C_o$ ) plotted versus a variable such as  $x$  or  $u$  were analyzed for the three model versions. The HEGADAS 3 + model showed few major trends in the residual plots except for a downtrend with distance,  $x$ , for the ERP/URA trials. The trends for the

Table 3

Summary of model performance measures for three HEGADAS model options applied to the Kit Fox data: HEGADAS 3 +, original HEGADAS 3.0, and HEGADAS 3 + (two roughnesses). MG is the geometric mean, VG is the geometric variance, FAC2 is the fraction of predictions within a factor of two of observations, and HIGH C is the highest concentration observed or predicted. A perfect model has  $MG = VG = FAC2 = 1.0$

	MG	VG	FAC2	HIGH C (ppmv)
Observed				98,700
HEGADAS 3 +	1.06	1.19	0.89	76,400
HEGADAS 3.0	0.49	2.00	0.52	652,900
HEGADAS 3 + (two roughnesses)	0.96	1.15	0.92	76,410

original HEGADAS 3.0 model closely paralleled those for the HEGADAS 3 + model, except that the HEGADAS 3.0 model indicated large overpredictions (by a factor of 2–4) for the puff trials. The residual plots for the HEGADAS 3 + (two roughnesses) model were the same as for the HEGADAS 3 + model for the URA trials. However, for the ERP/URA trials, the residual plots for the HEGADAS 3 + (two roughnesses) model indicated that the downward trend with distance had been removed. This trend disappeared for the HEGADAS 3 + (two roughnesses) model because a roughness of 0.12 m was used for the 25 and 50 m arcs, and a roughness of 0.035 m was used for the 100 and 225 m arcs. It is primarily because of this improvement that the relative scatter, VG, is slightly less in Fig. 2 for the HEGADAS 3 + (two roughnesses) model than for the HEGADAS 3 + model.

Table 3 contains a brief summary of the major results of the evaluations, including the geometric mean, MG, the geometric variance, VG, the fraction of predictions within a factor of two of observations, FAC2, and the highest concentration (in ppmv) observed and predicted. The MG and VG values have been plotted in Fig. 2 and discussed earlier. The FAC2 numbers indicate that 89% of the HEGADAS 3 + model predictions are within a factor of two of the observations, whereas only 49% of the HEGADAS 3.0 model predictions satisfy this criterion. The fraction improves slightly for HEGADAS 3 + (two roughnesses). The “HIGH C” column in Table 3 shows that the predictions of the HEGADAS 3 + model versions are close to the observation (about 23% low), while the prediction of the original HEGADAS 3.0 model is about 6.5 times higher than the observation and is 65% of pure  $CO_2$  gas.

It can be concluded that the HEGADAS 3 + model is able to satisfactorily simulate the concentrations observed at the Kit Fox experiments and has better

performance than the original HEGADAS 3.0 model. A slight improvement is offered in regions with strong variations in roughness if the HEGADAS 3 + model is run twice – once for receptors in the near-source area with higher roughness, and once for receptors in the more distant area with smaller roughness.

#### 4.3. Evaluation results for cloud width, height, and speed

The evaluations of the predictions of the maximum near-ground concentrations on a given monitoring arc, described in the previous section, are generally of most interest. However, it is also important that the model be able to accurately simulate cloud parameters such as cloud width and depth and cloud speed. Otherwise, there may be compensating errors that mask a fundamental problem with model physics.

Section 3 presented discussions of the observed Kit Fox cloud widths,  $\sigma_y$ , cloud heights,  $h(0.5)$ , and cloud advection speeds,  $u_c$ . The current section summarizes comparisons of these observations with the HEGADAS model predictions.

*Cloud width  $\sigma_y$ :* The HEGADAS 3 + model and the HEGADAS 3 + (two roughnesses) model tend to slightly overpredict  $\sigma_y$  by about 20% on average. The amount of the overprediction is largest, about 65%, for the continuous plumes in the ERP/URA roughness array. The HEGADAS 3.0 model overpredicts by a larger amount, about 40–50% on average.

*Cloud height  $h(0.5)$ :* All three model versions underpredict cloud height,  $h(0.5)$ , by over a factor of two, on average. The underprediction is largest, about a factor of three, for the ERP/URA trials, where it was shown in Section 3 that the observed cloud height was always about equal to or larger than the height of the ERP obstacles, 2.4 m. This underprediction tendency was also found for all dense gas dispersion models evaluated by Hanna et al. (1993).

*Cloud speed  $u_c$ :* When all data are considered, the HEGADAS 3 + model and the HEGADAS 3 + (two roughnesses) model do an excellent job of predicting cloud speed  $u_c$ . However, this excellent performance may be the result of compensation of a 30% underprediction for the ERP puffs by a 30% overprediction for URA continuous releases. The original HEGADAS 3.0 model overpredicts cloud speeds by 30–40% on average, but does quite well for the ERP puffs.

It is concluded that there may be some compensating errors occurring in the model, since it is seen to underpredict the cloud height and slightly overpredict the cloud width. However, in view of the fact that cloud heights are underpredicted by factors of two or three, it is puzzling that the cloud speeds are predicted fairly well. One would expect cloud speeds to be underpredicted if cloud heights were underpredicted. There are two reasons why this discrepancy in cloud heights may not have

a major effect on the concentration predictions. First, the “observed” cloud speed is not defined the same as the local cloud speed predicted by the model, but is an averaged cloud speed over the entire trajectory of the cloud (observed  $u_c$  is calculated as the downwind distance divided by the travel time from the source to the arc). Therefore, the observed cloud speed is expected to be less than the predicted local cloud speed. Second, the observed cloud speed is affected by the presence of the ERP and URA obstacles, whereas the model does not account at all for the flow in and around the roughness obstacles. As a result, the observed cloud speed for the deeper cloud turns out to be about the same as the predicted cloud speed for the shallower cloud.

## 5. Conclusions

The Kit Fox dense gas dispersion field experiment produced 52 separate cloud release trials that allow us to gain many insights into the physics of dense gas transport and dispersion over rough surfaces. This paper has described the field experiment, the highlights of the concentration and meteorology observations and their use in parameterizing model components, and the evaluation of the HEGADAS dense gas dispersion model.

As part of the PERF study a revised vertical entrainment formula (Eq. (2)) has been derived from the wind tunnel experiments described by Briggs et al. (2001). This revised formula was included in HEGADAS 3 + in a sensitivity run with the Kit Fox data, leading to the conclusion that the performance of the model was little changed. The new entrainment formula caused the model to underpredict slightly due to the 20% larger entrainment assumed for passive (neutral) clouds in Eq. (2). It is concluded that the original vertical entrainment formula in HEGADAS, similar to the formula in other widely used dense gas dispersion models, is performing adequately.

The Kit Fox data suggest that the along-wind dispersion coefficient,  $\sigma_x$ , is two times larger than the value assumed in the original HEGADAS 3.0 model. This finding agrees with Petersen’s (1992) wind tunnel data and with a comprehensive analysis of many field data reported by Hanna and Franzese (2000). Hanna and Chang (1995) used the Petersen (1992) data to develop the updated along-wind dispersion formula in the HEGADAS 3 + model. The Kit Fox model evaluation exercise verifies that the along-wind dispersion assumption by Hanna and Chang (1995) is satisfactory, although the sensitivity studies suggest that the predicted concentrations are not very sensitive to the exact form of the  $\sigma_x$  formulation.

The Kit Fox data verify the revised advective speed,  $u_c$ , algorithms in the HEGADAS 3 + model, which assumes an advective speed,  $u_c$ , that is 30% smaller than that in

the original HEGADAS 3.0 model (Hanna and Chang, 1995). The Kit Fox results show that the observed and predicted  $u_c$ 's tended to agree fairly well, with little bias. This result is important because it is found that the model predictions of concentration are sensitive to the cloud advection speed. The Kit Fox observations of  $u_c$  verify the model expectation that advection speeds will increase with downwind distance, due to the fact that the cloud grows vertically.

Because the predicted cloud heights,  $h(0.5)$ , tended to be a factor of two or three less than the Kit Fox observed cloud heights, it had been anticipated that the observed cloud advection speeds would be underpredicted. However, since the model does not account for the slowing of the wind at heights less than the obstacle height (2.4 m for the ERP and 0.2 m for the URA), the two effects may tend to cancel, causing good agreement in the resulting advection speeds.

The Kit Fox observed peak near-ground concentrations normalized by source emission rate,  $(C/Q)_{\max}$ , decrease strongly as surface roughness length increases. Observed  $(C/Q)_{\max}$  values over the ERP were about a factor of three to five less than those for the URA for both continuous releases and for puff releases. Observed  $(C/Q)_{\max}$  values over the URA were about three or four times less than those for the flat desert releases. A  $(C/Q)_{\max} \propto z_0^{-1/2}$  relation provided a good fit to all data. It is important to note that these  $(C/Q)_{\max}$  values generally occurred during similar meteorological conditions (light wind, stable conditions) for the three groups of experiments with different roughnesses. The HEGADAS model was able to satisfactorily simulate these observed strong variations of peak concentration with surface roughness length.

It was found that a simple method of accounting for a roughness change with distance is to run the model twice – once using the “close-in” roughness length for calculating concentrations at monitoring arcs influenced by that roughness length, and once using the “far-field” roughness length for calculating concentrations at monitoring arcs influenced by the lower roughness. When this method was used in the HEGADAS 3 + (two roughnesses) model, the predictions for the ERP/URA trials were improved.

Although the observed Kit Fox cloud heights,  $h(0.5)$ , were always greater than the obstacle height, the HEGADAS model predictions of cloud height at the closest (25 m) monitoring arc were sometimes less than  $\frac{1}{4}$  of the height of ERP obstacles. The HEGADAS model, like most other dense gas slab models, does not simulate the details of flow within the obstacle array and therefore does not account for the strong vertical mixing of the dense gas cloud within the recirculating cavity of the 2.4 m high ERP obstacles. Nevertheless, the model was able to satisfactorily simulate the maximum observed concentration, perhaps because of compensating errors

involving the wind speed at heights less than the obstacle heights.

The previous paragraphs emphasized model components such as cloud advective speed. The predicted and observed concentrations were also compared for all 52 trials and for the four downwind distances. The HEGADAS 3 + model modifications proposed by Hanna and Chang (1995) produced predicted concentrations that agree satisfactorily with the Kit Fox observations (less than 5% mean bias, scatter of less than 40%, and about 90% of predictions within a factor of two of observations). The original HEGADAS 3.0 (Witlox, 1994; Post, 1994) model tends to overpredict by a factor of two, in the mean, with larger overpredictions for the finite duration (puff) releases (as also found by Hanna and Chang (1995) in their evaluations of HEGADAS 3.0 with the Petersen (1992) wind tunnel data). A slight downward trend found in the residual plots with distance for the HEGADAS 3 + model for the ERP trials was removed by use of the assumption in the HEGADAS 3 + (two roughnesses) model, where the model should be run twice, once using the ERP roughness for the 25 and 50 m monitoring arcs, and once using the ERP/URA roughness for the 100 and 225 m monitoring arcs.

While the Kit Fox data all involve clouds with heights greater than the roughness elements, and while the model does not account for the altered wind profiles and greatly increased turbulence that probably would occur near the ground deep within a dense obstacle array, it is expected that the actual cloud transport and dispersion deep within obstacle arrays would be determined by two competing effects. The first effect involves the reduced dilution (and hence a tendency towards higher concentrations) associated with reductions in wind speed. The second effect involves the increased dispersion (and hence a tendency towards lower concentrations) associated with increases in turbulence intensity. The actual changes in concentration for clouds with heights much less than the obstacle height would depend on which of these competing effects is dominant.

#### Acknowledgements

Exxon Research and Engineering Company (ER&E) served as contract coordinator for this PERF 93-16 Project. Mr. Kenneth W. Steinberg of ER&E has been the project manager over the six-year duration of the project. Without his thorough and efficient management, all the components of the project would not have been satisfactorily completed. The other companies financially supporting the PERF 93-16 Dispersion Modeling project include Allied-Signal Incorporated, AMOCO Corporation, Chevron Research and Technology Company, Mobil Research and Development Company, Shell

Development Company, CITGO Petroleum Corporation, Clark Oil and Refining Corporation, Marathon Oil Company, and Phillips Petroleum Company. EPA has provided in-kind support through a Coordinated Research And Development Agreement (CRADA) with ER&E. DOE had provided financial support through their jointly sponsored research program with the Western Research Institute. In particular, Manny Vazquez of Allied-Signal, Douglas Blewitt of AMOCO, David Fontaine of Chevron, Gilbert Jersey of Mobil, Peter Roberts and John King of Shell, William Petersen and William Snyder of the EPA, Alan Robins and Ian Castro of the University of Surrey, Rex Britter of Cambridge University, and David Wilson of the University of Alberta have made numerous technical contributions. The field design plan and field experiments were largely the responsibility of WRI, with David Sheesley as project manager and Bruce King as field test technical manager. DRI played a large part in the concentration measurements at the field site, with John Bowen as field test technical director.

## References

- Briggs, G.A., Britter, R.E., Hanna, S.R., Havens, J.A., Robins, A.G., Snyder, W.H., 2001. Dense gas vertical dispersion over rough surfaces: results of wind tunnel studies. *Atmospheric Environment* 35, 2265–2284.
- Britter, R.E., McQuaid, J., 1988. Workbook on the dispersion of dense gases. HSE Contract Report Number 17/1988, HSE, Sheffield, England.
- Coulombe, W., Bowen, J., Egami, R., Freeman, D., Sheesley, D., Nordin, J., Routh, T., King, B., 1999. Characterization of carbon dioxide releases: experiment two. DRI Doc. No. 97-7240.1D, DRI, POB 60220, Reno, NV 89506-0220.
- Davidson, M.J., Mylne, K.R., Jones, C.D., Phillips, J.C., Perkins, R.K., Fung, J.C.H., Hunt, J.C.R., 1995. Plume dispersion through large groups of obstacles – a field investigation. *Atmospheric Environment* 29, 3245–3256.
- Goode, K., Belcher, S.E., 1999. On the parameterization of the effective roughness length for momentum transfer over heterogeneous terrain. *Boundary Layer Meteorology* 93, 133–154.
- Hanna, S.R., Chang, J.C., 1995. Analysis of dispersion of finite duration releases of dense gases and recommended revisions to HEGADAS. Earth Tech. Report No. 1411, prepared for Exxon Research and Engineering, 180 Park Ave., Florham Park, NJ 07932.
- Hanna, S.R., Chang, J.C., 1999. Testing of the HEGADAS Model using the Kit Fox field data. Proceedings of International Conference and Workshop on Modeling the Consequences of Accidental Releases of Hazardous Materials, 28 September–1 October 1999, San Francisco. ISBN-0-8169-0781-1, Center for Chemical Process Safety of the American Institute of Chemical Engineers, New York, NY, USA, pp. 229–246.
- Hanna, S.R., Chang, J.C., Briggs, G.A., 1999. Dense gas dispersion model modifications and evaluations using the Kit Fox field observations. Hanna Consultants Report No. P011F for API, 110pp. + appendices.
- Hanna, S.R., Franzese, P., 2000. Along wind dispersion – a simple similarity formula compared with observations at 11 field sites and in one wind tunnel. *Journal of Applied Meteorology* 39, 1700–1714.
- Hanna, S.R., Steinberg, K.W., 2001. Overview of Petroleum Environmental Research Forum (PERF) dense gas dispersion modeling project. *Atmospheric Environment* 35, 2223–2229.
- Hanna, S.R., Chang, J.C., Strimaitis, D.G., 1993. Hazardous gas model evaluation with field observations. *Atmospheric Environment* 27A, 2265–2281.
- Macdonald, R.W., Griffiths, R.F., Cheah, S.C., 1997. Field experiments of dispersion through regular arrays of cubic structures. *Atmospheric Environment* 31, 783–795.
- Petersen, R.L., 1992. Wind tunnel and HEGADAS simulations of Finite duration releases for a specific refinery with uniform roughness. Report 91-9782 by CPP, 1415 Blue Spruce Dr., Ft. Collins, CO 80524.
- Petersen, R.L., Cochran, B.C., 1995. Wind tunnel determination of equivalent refinery roughness patterns. CPP Report 94-1152 (Part I dated February 1995 and Part II dated July 1995), CPP, 1415 Blue Spruce Drive, Fort Collins, CO 80524.
- Post, L. (Ed.), 1994. HGSYSTEM 3.0 Technical Reference Manual. TNER.94.059. Shell Research Limited, Thornton Research Centre, P.O. Box 1, Chester, UK.
- Snyder, W.H., 1995. Wind tunnel roughness array tests. ASMD/NOAA, Research Triangle Park, NC 27711, 43pp.
- Western Research Institute (WRI), 1998. Final Report on the 1995 Kit Fox Project, Vol. I – Experiment Description and Data Processing, and Vol. II – Data Analysis for Enhanced Roughness Tests. WRI, Laramie, Wyoming, 109pp + 67pp.
- Witlox, H.W.M., 1994. The HEGADAS model for ground-level heavy-gas dispersion – II. Time dependent model. *Atmospheric Environment* 28, 2933–2945.